Science of the Total Environment 849 (2022) 157924

Contents lists available at ScienceDirect

Science of the Total Environment

journal homepage: www.elsevier.com/locate/scitotenv

Impacts of invasive mussels on a large lake: Direct evidence from in situ control-volume experiments

Zhiqiang Xia [a,*], David C. Depew [b], Reza Valipour [b], Hugh J. MacIsaac [a,c], R. Paul Weidman [a,*]

[a] Great Lakes Institute for Environmental Research, University of Windsor, Windsor, ON N9B 3P4, Canada
[b] Environment & Climate Change Canada, Watershed Hydrology & Ecology Research Division, Burlington, ON L7R 4A6, Canada
[c] School of Ecology and Environmental Science, Yunnan University, Kunming 650091, China

HIGHLIGHTS

- In situ grazing rates of quagga mussels were measured in control volume experiments.
- Grazing was restricted to the zone 0.1–0.5 m from lake bottom.
- Grazing calculated in the horizontal direction agreed with vertical depletion of lake seston.
- Grazing was affected by flow, depth, seston concentration, and stoichiometric ratios.
- Grazing on P exceeded that on C and N, supporting the nearshore P-shunt hypothesis.

GRAPHICAL ABSTRACT

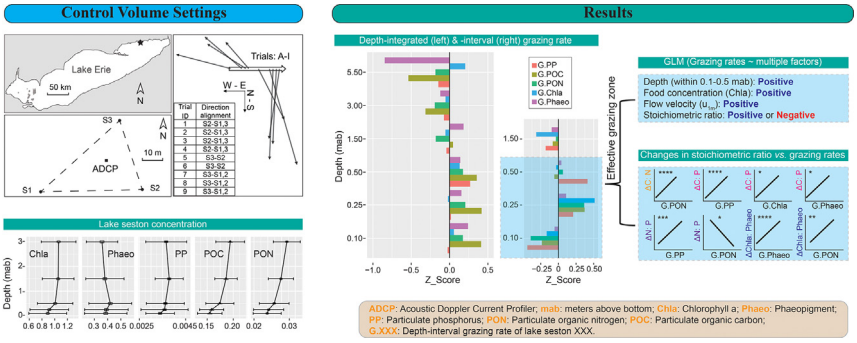

ARTICLE INFO

Editor: Julian Blasco

Keywords:
Dreissena
Great Lakes
Phosphorus
Flow velocity
Ecological stoichiometry
Control volume

ABSTRACT

Invasive dreissenid mussels have reengineered many freshwater ecosystems in North America and Europe. However, few studies have directly linked their filter feeding activity with ecological effects except in laboratory tests or small-scale field enclosures. We investigated in situ grazing on lake seston by dreissenid mussels (mainly quagga mussel *Dreissena rostriformis bugensis*) using a 'control volume' approach in the nearshore of eastern Lake Erie in 2016. Flow conditions were measured using an acoustic Doppler current profiler, surrounded by three vertical sampling stations that were arranged in a triangular configuration to collect time-integrated water samples from five different depths. Seston variables, including chlorophyll *a*, phaeopigment, particulate organic carbon and nitrogen, and particulate phosphorus, along with stoichiometric ratios and water flow over mussel colonies, were considered when estimating grazing rates. We observed suboptimal flow velocity for mussel grazing, i.e., 0.028 m s^{-1} at 0.1 m above bottom (mab), and resuspension was deemed minimal. Water temperature (mean: 25.1 °C) and an unstratified water column were optimal for grazing. Concentration of seston was low (mean: 0.2 mg L^{-1} particulate organic carbon) and decreased from surface to lakebed where noticeable depletion was observed. Grazing rates calculated at discrete depths varied substantially among trials, with maximum rates occurring at 0.25 or 0.5 mab. Positive grazing rates were restricted to 0.5 mab and below, defining an effective grazing zone (0.1–0.5 mab) in which the flow velocity, seston concentration, and water depth were consistently and positively correlated with grazing rates of different lake seston variables. Horizontal changes in stoichiometric ratios of seston were strongly associated with grazing rates, revealing higher uptake of particulate phosphorus than nitrogen and carbon. Our study supports the nearshore phosphorus shunt hypothesis, which posits that dreissenid mussels retain phosphorus on the lake bottom and contribute to a wide range of ecological effects on freshwater ecosystems.

* Corresponding authors.
E-mail addresses: xiab@uwindsor.ca (Z. Xia), paul.weidman@uwindsor.ca (R.P. Weidman).

http://dx.doi.org/10.1016/j.scitotenv.2022.157924
Received 3 March 2022; Received in revised form 15 July 2022; Accepted 5 August 2022
Available online 8 August 2022

1. Introduction

Dreissenid mussels – zebra mussel (*Dreissena polymorpha*) and quagga mussel (*Dreissena rostriformis bugensis*) – are notorious invasive, epifaunal bivalves in many European and North American freshwater ecosystems, including the Laurentian Great Lakes (Strayer, 2009; Higgins and Vander Zanden, 2010). These mussels have caused enormous economic losses due to severe fouling of infrastructure (Connelly et al., 2007; Strayer, 2009). They have also reengineered invaded ecosystems through numerous effects, such as increased water transparency due to filtration of suspended matter (MacIsaac, 1996; Hecky et al., 2004; Strayer, 2009; Higgins and Vander Zanden, 2010; Burlakova et al., 2021; Li et al., 2021). Their filter-feeding activities couple pelagic and benthic environments (MacIsaac et al., 1992; Ackerman et al., 2001), resulting in transfer of suspended organic and inorganic material to the benthos (Conroy et al., 2005; Fera et al., 2017; Vanderploeg et al., 2017), thereby altering nutrient cycling and energy flow (Higgins and Vander Zanden, 2010; Williamson and Ozersky, 2019; Li et al., 2021). These influences have led to the nearshore phosphorus (P) shunt hypothesis, which describes the redirection of P fluxes from pelagic to nearshore regions by dreissenid mussels following their establishment (Hecky et al., 2004; Ozersky et al., 2015). High-density mussel populations are capable of sequestering large quantities of nutrients such as N and P and dramatically altering biogeochemical cycles of invaded ecosystems (Williamson and Ozersky, 2019; Li et al., 2021). Depending on food availability, quality, and palatability, suspended particles captured by mussels can be rejected as pseudofeces without being digested or consumed and assimilated, leading to altered nutrient stoichiometry of solid particles and soluble nutrients in invaded waters (Higgins and Vander Zanden, 2010; Vanderploeg et al., 2017; Williamson and Ozersky, 2019). Improved light penetration can stimulate benthic algae or macrophyte growth in deeper areas (MacIsaac, 1996; Hecky et al., 2004), and selective grazing on phytoplankton communities may increase relative abundance of toxic species (Vanderploeg et al., 2001; Naddafi et al., 2007; Benelli et al., 2019). These changes have been attributed, in part, to the resurgence of harmful algal blooms and proliferation of nuisance benthic algae in the Great Lakes following the earlier success of P abatement projects (Hecky et al., 2004; Watson et al., 2016). In addition, the large-scale colonization of deeper regions of the Great Lakes by quagga mussels may pose even stronger impacts on food webs, biogeochemical processes, and water quality (Fera et al., 2017; Williamson and Ozersky, 2019; Burlakova et al., 2021; Li et al., 2021).

The overall impact of dreissenid mussels on aquatic ecosystems is influenced by a variety of factors related to their population characteristics (e.g., mussel density and size distribution) and to lake characteristics (e.g., mixing conditions, primary productivity) (MacIsaac et al., 1992; Ackerman et al., 2001; Conroy et al., 2005; Higgins and Vander Zanden, 2010; North et al., 2012; Vanderploeg et al., 2017; Williamson and Ozersky, 2019). Filtering abilities of dreissenid mussels and potential impacts on large ecosystems have been extrapolated from laboratory chambers (MacIsaac et al., 1992; Conroy et al., 2005; Xia et al., 2021) and field enclosures (Heath et al., 1995; Vanderploeg et al., 2017), while experimental field studies have been conducted less commonly (e.g., MacIsaac et al., 1999; Ackerman et al., 2001; Gergs and Rothhaupt, 2008). Studies in small-scale systems are suitable for exploring theoretical metrics (e.g., Coughlan, 1969; Jørgensen et al., 1990; Xia et al., 2020, 2021) and testing specific hypotheses associated with the filtering behavior of mussels (e.g., MacIsaac et al., 1992; Bayne et al., 1993; Conroy et al., 2005; Bykova et al., 2006; Vanderploeg et al., 2017;). However, whether these studies accurately depict events at much larger scales, especially in large lakes, remains to be determined. For example, the magnitude of suspended-particle redirection by dreissenid mussels is influenced by water depth, mixing, food concentration and quality, and water temperature (Ackerman et al., 2001; Ozersky et al., 2015; Vanderploeg et al., 2017; Xia et al., 2021). These conditions, especially complicated mixing patterns, are very hard to simulate in laboratory-based studies. As a result, studies in small-scale systems might tend to overestimate or underestimate the net effects of mussels, depending on experimental settings (e.g., Ozersky et al., 2015; Xia et al., 2021). The Great Lakes are experiencing appreciable replacement of zebra mussels by quagga mussels and the latter can colonize even deeper water, which is further complicating our understanding of their ecological impacts (Karatayev et al., 2021, 2022) and requires field-based studies. Further investigation of the multiple factors that regulate in situ grazing rates of dreissenid mussels is needed to better inform ecosystem impact assessments and nutrient management in large lakes (Sterner et al., 2017; Sterner, 2021).

Generally, impacts of dreissenid mussels are positively regulated by water column mixing since mussels rely on currents to replenish food supply (MacIsaac et al., 1999; Ackerman et al., 2001; Xia et al., 2021; Jabbari et al., 2021). The most obvious direct impact of dreissenids is the formation of a seston-depleted layer near mussel beds when mixing is weak, while stronger mixing results in a greater reduction of total lake seston (MacIsaac et al., 1999; Ackerman et al., 2001; Boegman et al., 2008; Mosley and Bootsma, 2015; Shen et al., 2020). However, quantifying the effects of the multiple aforementioned parameters on in situ grazing rates is required to inform whole-lake estimates of mussel grazing impacts (e.g., Boegman et al., 2008; Mosley and Bootsma, 2015; Shen et al., 2020; Li et al., 2021).

Although in situ measurements of bivalve grazing rates are challenging due to the difficulty of making direct observations on the bottom of lakes, the control volume approach has been used successfully in marine field studies to quantify flux of materials in coastal regions (e.g., Genin et al., 2009; Wyatt et al., 2010). For example, this method has been used to estimate coastal nutrient fluxes across coral reefs in places where relatively simple and consistent current conditions (e.g., unidirectional flow) were present (e.g., Genin et al., 2009; Wyatt et al., 2010). This approach involves the deployment of sampling equipment in a conceptual box at the study site by constructing four sampling stations, each consisting of an array of sampling pumps across the water column. Discrete samples from different depths can be used to estimate the cross-column concentration of lake seston. Every two neighboring strings form a virtual wall, and the water surface is regarded as the ceiling of the imaginary box. Along with unidirectional flow, the net nutrient flux can be estimated based on a simplified mass-balance model, where the mass difference between walls through which nutrients flow into (i.e., affluence) and out of (i.e., effluence) is considered a result of benthic filtration (Genin et al., 2009). The vertical flux from the water surface is assumed to be negligible, while resuspension can be considered when necessary. In the horizontal dimension, the mass difference can be calculated by multiplying the concentration difference between affluence and effluence stations (i.e., upstream-downstream stations along the flow direction path) by the volumetric flow rate (Wyatt et al., 2010). In terms of quantifying the flux of chlorophyll *a*, which is an indicator of primary production, algal growth rate is often assumed to be negligible due to the short timescale (e.g., hourly) of these estimates (Wyatt et al., 2010).

The objective of this study was to investigate the effects of multiple environmental factors on in situ grazing rates of lake seston by quagga mussels in nearshore regions of the Great Lakes. As a novel application in freshwater ecosystems, we expected that the control volume approach could be used to estimate the fluxes of lake seston associated with grazing activities of benthic mussels, which would provide a direct test of the nearshore P shunt hypothesis. Specifically, we hypothesized that: 1) grazing rates derived from the control volume approach would increase towards the lake bottom in agreement with the vertical distribution of lake seston observed over mussel reefs; and 2) grazing by mussels would deplete the P-content of lake seston, consistent with the nearshore P shunt hypothesis (Hecky et al., 2004) and ecological stoichiometric theory (Elser et al., 2000; Frost et al., 2002).

2. Materials and methods

2.1. Study area

We carried out the control volume experiments on August 8–11, 2016, at a nearshore site located in the eastern basin of Lake Erie in Ontario,

Canada (42°49′5.16″N, 79°42′12.27″W) (Fig. 1A). This site was ~4 km from the shoreline and was ~6 m deep. Mussel density at the study area was 4624 ± 313 (mean ± SD) individuals m^{-2}, with mean biomass of 70.1 g shell-free dry weight m^{-2} (Table 1), which was sampled in three random 0.15 m^2 quadrats within the control volume by SCUBA divers before the experiment (i.e., July 12, 2016; Depew, unpublished data). Biomass of benthic macroalgae *Cladophora glomerata*, which was surveyed at the same sites as mussels was ~63 g wet weight m^{-2}, although maximum biomass was expected at <2.0 m depth due to light limitation near the lake bottom (Higgins et al., 2006).

2.2. Physical condition measurements

The flow direction at the study site was multidirectional but predominantly from east to west under the influence of wind-driven currents, although episodic currents from the west influence coastal upwelling events in this area (Valipour et al., 2019). Flow conditions at this site made it challenging to quantify in situ measurements of grazing rates of lake seston by dreissenid mussels. To solve this, we deployed an unattended, downward-facing, tripod-mounted, acoustic Doppler current profiler (ADCP), which is widely used in marine and freshwater ecosystems to profile current conditions, to record horizontal flow rates at different depths (bin size: 0.1 m). The ADCP measured flow rates in the east to west (E-W) and north to south (N-S) directions, which were used to calculate the magnitude and direction of flow, which were positive to the east and the north, respectively. The downward-facing 2 MHz pulse coherent ADCP was programmed to burst record flow velocity from 1.7 m above the bottom (mab) to the bed every 5 min at 2 Hz over 256 s in 2 cm bins towards the bed (accuracy ± 1 % of measured values). The mean of these records at each 5 min burst was used to calculate the depth-averaged horizontal flow velocity (u_r). Observed velocity at lake bottom (i.e., deepest value at the velocity profile) was recorded as $u_{r.z0}$, and velocity at 1.0 mab as u_{1m}. To estimate mixing conditions at the lakebed, we estimated bottom shear velocity (u_*) by least-square fitting the law of the wall equation following the method of Valipour et al. (2015):

$$u_z = \frac{u_*}{K} \ln\left(\frac{Z}{Z_0}\right) \quad (1)$$

in which u_z is flow velocity at height Z above bottom, K is the von Karman constant (0.41), Z_0 is the hydraulic roughness or roughness length (m).

In addition, drag coefficient, C_D, which relates shear velocity and bottom stress, was estimated following Monismith et al. (2010):

$$C_D = \frac{u_*^2}{u_{1m^2}} \quad (2)$$

We then used the flow velocity at 1.0 mab to estimate the Z_0, thus,

$$Z_0 = exp\ \frac{-u_{1m}K}{u_*} \quad (3)$$

To ensure quality fitting of the law of the wall, we retained only estimated values for u_*, C_D, and Z_0 for observations with $u_r > 0.01$ m s^{-1} in the data analysis (Lorke et al., 2002; Valipour et al., 2015).

Vertical wave height (VWH) was measured by a buoy deployed by Fisheries and Oceans Canada nearby in the east basin of Lake Erie (DFO-MSC buoy No. 45142). Water temperature was measured every minute at nine different depths (1.0–5.0 mab at 0.5 m intervals) using Tidbit data loggers (Onset Inc., MA, USA; accuracy of ±0.1 °C) deployed at the center of the control volume study area. Wind speed in the study area was retrieved from a meteorological buoy located at ~35 km east of the study location (Depew et al., 2006).

2.3. Control volume settings and sample collection

We considered relatively short-term (~1 h) trials to ensure unidirectional flow because a priori knowledge of flow direction was not available. We set three (originally four, but one failed due to an electronic problem) sampling stations (strings) surrounding the ADCP, so that post hoc determination of a pair of affluence-effluence stations was possible (Fig. 1B). Although one station was missing, only two sampling stations (i.e., affluence and effluence) are required to estimate the flux when relatively homogenous or confined flow conditions are present (Genin et al., 2009; Wyatt et al., 2010). Such a modification in our study did not preclude the use of three sampling stations because once the flow direction was known the affluence-effluence station pairs and corresponding lake seston concentrations and flow distance could be calculated.

We constrained our estimation of lake seston flux (i.e., grazing rate) by considering a unit width (1.0 m) of bottom surface, which was selected for computing ease, between the affluence and effluence stations. Specifically, depending on the alignment between flow direction and sampling stations, we considered one downstream string as an effluence station when the flow direction was approximately parallel with the two stations (i.e., trials E–I in Fig. 1C). Otherwise, both two downstream strings were used to determine

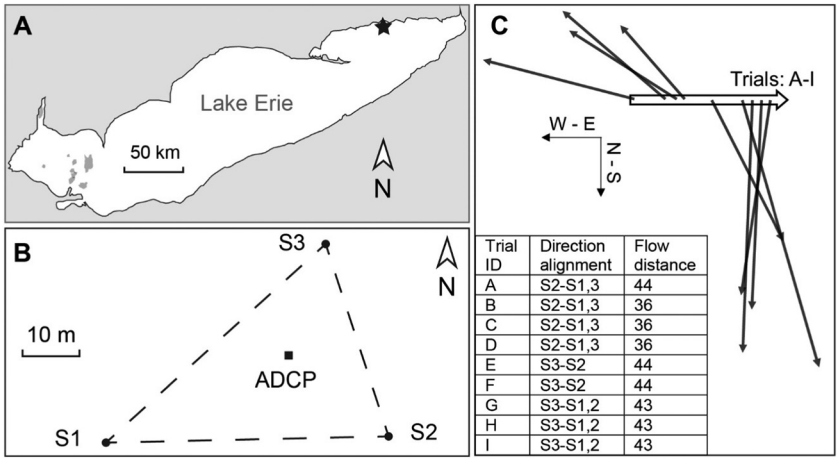

Trial ID	Direction alignment	Flow distance
A	S2-S1,3	44
B	S2-S1,3	36
C	S2-S1,3	36
D	S2-S1,3	36
E	S3-S2	44
F	S3-S2	44
G	S3-S1,2	43
H	S3-S1,2	43
I	S3-S1,2	43

Fig. 1. Sampling map and flow information of the study, showing (A) the study location (filled star) in Lake Erie, (B) location of three sampling stations and the ADCP recorder, and (C) the flow directions and relative flow velocities of nine trials. The trials are ordered by the approximate experimental time, and the length of arrows corresponds to flow rates. The table in panel C demonstrates alignment between flow direction and sampling stations, and corresponding flow distance in the subsequent calculations.

Table 1
Summary of experimental settings, showing the mean (SD) and range of different variables and their definitions. mab = meters above bottom.

Category	Variable	Unit	Mean (SD)	Range	Definition
Habitat information	Mussel density	Individuals m^{-2}	4624 (313)	4340–4960	Mussel abundance per m^2 surface of lakebed
	Mussel biomass	g	70.1(8.2)	64.0–79.4	Mussel shell-free dry weight per m^2 surface of lakebed
	Water temperature	°C	25.1 (0.6)	24.4–26.7	Water temperature at nine depths (1–5 mab) foreight trials
Study Implementation	Duration	min	54 (10)	45–70	–
	Time of day	–	–	9:50–18:00	–
	Flow distance	m	41 (4)	36–44	Distance between affluent and effluent stations aligned with flow directions
	Residence time	min	20.0 (5.4)	12.7–29.8	Calculated as flow distance divided by u_r
Climate and flow dynamics	Wind speed	m s^{-1}	3.9 (1.9)	0.4–8.8	–
	Wave height	m	0.26 (0.16)	0.00–0.70	–
	Peak wave period	s	3.1(0.5)	2.0–4.3	–
	$u_{r.z0}$	m s^{-1}	0.0281 (0.0380)	0.0001–0.2013	Horizontal flow velocity at 0.1 mab
	u_{1m}	m s^{-1}	0.0439 (0.0198)	0.0005–0.1035	Horizontal flow velocity at 1.0 mab
	u_r	m s^{-1}	0.0370 (0.0119)	0.0029–0.0867	Depth-average horizontal flow velocity within 0.1–1.7 mab
Lake seston	Chla	μg L^{-1}	0.998 (0.275)	0.366–1.431	Chlorophyll a
	Pheao	μg L^{-1}	0.382 (0.141)	0.122–0.746	Phaeopigment
	PP	mg L^{-1}	0.004 (0.001)	0.002–0.005	Particulate phosphorus
	PON	mg L^{-1}	0.028 (0.006)	0.016–0.040	Particulate organic nitrogen
	POC	mg L^{-1}	0.177 (0.029)	0.113–0.244	Particulate organic carbon
Stoichiometric ratio	C: N	–	7.4 (0.5)	5.9–8.7	Molar POC: PON
	C: P	–	137.6 (35.1)	83.2–228.5	Molar POC: PP
	N: P	–	18.8 (4.9)	10.9–32.3	Molar PON: PP
	Chla: Phaeo	–	3.0 (1.1)	1.7–7.3	Mass Chla: Phaeo

the affluence station and the lake seston concentration (i.e., trials A–D & G–I in Fig. 1C). For each trial, the volumetric flow rate per unit lakebed (i.e., mussel bed) width (m^2 s^{-1}) was calculated as:

$$q = u_r H \tag{4}$$

in which the u_r is the depth-averaged flow velocity (in m s^{-1}) across the mussel bed as described above, and H is the local water depth (m).

The three sampling stations were placed approximately 40–50 m apart, surrounding the ADCP (Fig. 1B). Each station consisted of a buoy and five sampling units mounted at different depths (i.e., 0.1, 0.25, 0.5, 1.5, 3.0 mab) on a string suspended from a floating buoy. Each sampling unit consisted of a 2 L intravenous infusion bag and a 12 V DC impeller pump, which pumped lake water into the bag. We used drip irrigation fittings to reduce the flow into the bag and thus facilitated the collection of a time-integrated sample to reduce natural variability when collecting discrete samples (Genin et al., 2009). We covered the intake of each infusion bag with a 2-mm mesh filter to prevent collecting large detritus that could affect chemical measurements. Water samples were stored in the dark on ice, filtered onto 25 mm GF/C filters within 1 h of collection, and transported to laboratory within 6 h of collection. We ran a total of nine trials from August 9–11 (day 221–224 of the year), with each lasting 45–70 min (Table 1).

2.4. Seston concentrations and mussel grazing rates

Water samples were assessed for total chlorophyll *a* (Chla), phaeopigment (Phaeo), particulate phosphorus (PP), particulate organic nitrogen and carbon (PON and POC, respectively), and considered each a proxy of lake seston concentration in the subsequent analysis since they were all positively correlated (Table 2). Filters for measurement of POC/PON and PP were submitted to the National Laboratory for Environmental Testing (NLET, Burlington, ON). Filters for Chla and Phaeo were measured by fluorometric analysis. At each station, depth-integrated seston concentrations were calculated as:

$$C = \frac{1}{H} \times \Sigma_1^6 C_i \times H_i \tag{5}$$

where C_i is the concentration at the ith discrete layer, and H_i is the water depth of the ith discrete layer. Here we also included the layer between 3.0 mab and surface while the concentration was not measured but assigned the same as at 3.0 mab (see below). The average concentration of lake seston for the entire control volume was calculated as the mean of the three stations.

Depth-integrated mussel grazing rates of lake seston (G_{intg}) were calculated, through the control volume with depth H in the horizontal direction (mg m^{-2} h^{-1} or μg m^{-2} h^{-1} depending on the variable of interest), as the total flux of lake seston (J_{total}) into the control volume, i.e.,

$$G_{intg} = J_{total} = 3.6 \times 10^6 \times q_{intg} \times \frac{\Delta C_{intg}}{\Delta X} \tag{6}$$

where q_{intg} is the volumetric flow rate per unit mussel bed width in eq. 4, calculated using the depth of the entire water column; $\Delta C_{intg} = (C_{intg.afl} - C_{intg.efl})$ is the difference of depth-integrated concentration of lake seston (mg L^{-1} or μg L^{-1}) between affluence and effluence stations. Thus, a positive value indicated net grazing of lake seston by mussels from the water flowing over the mussel colonies; $\Delta X = |X_{afl} - X_{efl}|$ is the distance (m) between affluence and effluence stations, and the constant (3.6×10^6) was used to unify the units among components. When two stations were used to determine an effluence station (i.e., trials A–D & G–I in Fig. 1C), the average concentration was used as C_{efl}. The concentration of lake seston in the surface layer (i.e., 5.5 mab) was not measured and was assumed to equal concentration at 3.0 mab.

Table 2
Correlation coefficients (Pearson *r*) between variables of lake seston and flow conditions within the 0.1–1.98 mab zone. Significance level: ** = 0.01, *** = 0.001, **** = 0.0001.

		Chla	Phaeo	PP	PON	POC
Lake seston	Chla	1.00				
	Phaeo	0.82****	1.00			
	PP	0.59****	0.42**	1.00		
	PON	0.60****	0.23	0.53***	1.00	
	POC	0.75****	0.46**	0.54***	0.91****	1.00

		u_r	u_{1m}	$u_{r.z0}$	u_*	Z_0	C_D
Flow condition (0.1–1.98 mab)	u_r	1.00					
	u_{1m}	0.99***	1.00				
	$u_{r.z0}$	0.17***	0.26***	1.00			
	u_*	0.69***	0.76***	0.73***	1.00		
	Z_0	0.19***	0.28***	0.98***	0.76***	1.00	
	C_D	0.19***	0.27***	0.97***	0.77***	0.99***	1.00

We also calculated grazing rates of lake seston by mussels at each interval depth (i.e., depth-interval grazing rates, G) as:

$$G = 3.6 \times 10^6 \times q_{intv} \times \frac{\Delta C_{intv}}{\Delta X} \quad (7)$$

where ΔC_{intv} is the concentration difference of lake seston between affluence and effluence stations at the respective depth from lake bottom. To reduce potential impacts of natural sedimentation on G, we considered the 3.0 mab depth a control to correct the ΔC_{intv} because we expected that within the experimental duration (~1 h) the 3.0 mab layer was beyond direct influence of mussel grazing. Therefore, ΔC_{intv} was calculated as $\Delta C_{intv} = (C_{afl} - C_{efl}) - (C_{afl}' - C_{efl}')$, in which the $(C_{afl} - C_{efl})$ is the concentration difference between affluence and effluence stations at each depth, and $(C_{afl}' - C_{efl}')$ was calculated at 3.0 mab (i.e., control). To simplify estimation, we considered a control volume with a unit depth of 1 m at each interval depth to estimate the q_{intv} in Eq. (7).

We also calculated changes in stoichiometric ratios of lake seston between affluence and effluence stations at each interval depth, also considering the 3.0 mab depth a control layer, i.e.,

$$\Delta Ratio = \left(Ratio_{efl} - Ratio_{afl}\right) - \left(Ratio_{efl}' - Ratio_{afl}'\right) \quad (8)$$

2.5. Statistical analysis

Relationships between variables of lake seston concentrations or between flow conditions were examined using Pearson correlation tests. The overall vertical distribution of lake seston concentrations within 0.1–3.0 mab was investigated using linear mixed effect models (LMMs) using R package '*nlme*' (Pinheiro et al., 2021) that related each lake seston concentration to depth (Ln transformed) because observations at each depth were nested within a trial (Zuur et al., 2009). We considered depth as a fixed effect and trial as a random effect in models and used the AIC (Akaike Information Criterion) and likelihood ratio test to determine the best random structure (i.e., random intercept vs. random intercept and slope) (Zuur et al., 2009). The same method was used to investigate stoichiometric ratios of lake seston at each depth in the water column, and data was Ln or Log_{10} transformed to improve normality when necessary.

We used a Friedman test, followed by a Wilcoxon signed-rank test for post hoc pairwise comparisons (R package '*rstatix*', Kassambara, 2021) to identify any significant differences in lake seston concentrations, grazing rates, stoichiometric ratios, and corresponding changes in these parameters between affluence and effluence stations among depths within the 0.1–3.0 mab zone. In addition, Z-transformed standard deviates of depth-interval grazing rates (0.1–1.5 mab) and depth-integrated grazing rates (0.1–5.5 mab) were calculated for each trial to better assess differences among depths (Ackerman et al., 2001).

We modeled the depth-interval grazing rates of lake seston as a function of multiple environmental factors to explore potential regulators, which consisted of four categories: hydraulic flow conditions (i.e., u_r, $u_{r.z0}$, u_{1m}, C_D, and u_*), food concentration (Chla, Phaeo, PP, PON, and POC), stoichiometric ratios of lake seston (Chla: Phaeo, POC: PON, POC: PP, and PON: PP, hereafter Chla: Phaeo, C: N, C: P, and N: P, respectively), and water depth above the bottom. These models were focused on a data subset for the near-bottom region (0.1–0.5 mab) because this represented a presumed effective grazing zone of the mussels (see results and discussion). We used multiple linear regressions following a preliminary comparison with mixed effect models (Zuur et al., 2009). We controlled for multicollinearity among predictors by removing variables with the highest variance inflation factors (VIF) in a stepwise manner ('*car*' R package; Fox and Weisberg, 2019) until all VIFs were no >5.0 (Zuur et al., 2010). We then reduced the model by conducting an AIC-based variable selection in both directions (i.e., forward and backward), with the resulting models validated by examining default diagnostic plots. To compare the relative importance of variables retained in models, we standardized all variables before modeling.

We conducted a pairwise correlation analysis between depth-interval grazing rates and depth-interval stoichiometric changes of lake seston for 0.1–0.5 mab zone to examine their relationships. All statistical analyses were performed using R (version 4.0.3, R Core Team, 2020).

3. Results

3.1. Climatic and hydrodynamic conditions

During the field campaigns, the average wind speed was 3.9 m s^{-1} (range: 0.4–8.8) and vertical wave height was 0.26 m (0–0.7) with a peak wave period of 3.1 s (2.0–4.3) (Table 1). Average water temperature was 25.1 °C, ranging from 24.4 to 26.7 °C among trials (Table 1). There was no evidence of thermal stratification during the study, although the last four trials had slightly greater differences in water temperature among depths (trials F–I, 1.1–1.6 °C) than did earlier trials (A–E, 0.8–1.0 °C; Fig. S1, supporting information). These patterns in water temperature agreed with reduced wind and wave intensities in the later trials (Fig. 2A,B).

Water flow was multidirectional among trials, with the first four (trials A–D) dominated by SE-NW flows and by N-S direction in the remaining trials (i.e., nearshore-offshore; Fig. 1C). Horizontal flow velocities at 1.0 mab (u_{1m}: 0.0439 m s^{-1}) were significantly correlated with cross-depth (i.e., averaged across all depths) velocity (u_r: 0.0370 m s^{-1}; Table 1) (r = 0.99; Table 2, Fig. 2C, D). Flow velocity at lake-bottom ($u_{r.z0}$: 0.0281 m s^{-1}) was lower than and only weakly related to the u_{1m} and u_r (r = 0.17–0.26; Table 2, Fig. 2E); however, $u_{r.z0}$ was more closely related to shear velocity (u_*: median = 0.0031 m s^{-1}), roughness height (Z_0: median = 0.0106 m), and drag coefficient (C_D: median = 0.0072; Fig. 3D–F) (r = 0.73–0.97; Table 2). Temporal variation of shear velocity (u_*), roughness height (Z_0), and drag coefficient (C_D) was approximately synchronous (Fig. 3A–C), as these variables were strongly correlated with each other (r = 0.76–0.99; Table 2). The Z_0 and C_D were approximately log-normal distributed (Fig. 3E-F), consistent with a previous study in central Lake Erie (Valipour et al., 2015).

3.2. Vertical distribution of lake seston and stoichiometric ratios

Average concentrations of Chla, Phaeo, POC, PON, and PP were 0.998, 0.382 μg L^{-1}, 0.177, 0.028 and 0.004 mg L^{-1}, respectively (Table 1). Most of these variables showed significant positive relationships (except Phaeo and PON, r = 0.23, $p > 0.05$; Table 2). Concentrations of Chla, PON, and POC decreased significantly with depth towards the lake bottom ($p < 0.05$, Fig. S2A, D, E, supporting information), whereas Phaeo and PP were not significantly correlated with depth (p = 0.096–0.578, Fig. S2B, C). In addition, concentrations of Chla and POC at 0.1 mab were significantly lower than that at 1.5 and 3.0 mab (Wilcoxon signed-rank test, $p < 0.05$), suggesting significant depletion of lake seston immediately above the lake bottom (Fig. 4).

The mass ratio of Chla: Phaeo and molar ratios of C: P and N: P decreased significantly with water depth towards the lake bottom (LMMs; p = 0.002–0.012; Fig. S3A, C, D, supporting information), while the molar ratio of C: N did not change (p = 0.176, Fig. S3B). Chla: Phaeo ratio at 0.25 and 0.5 mab was significantly lower than at 1.5 and 3.0, and 3.0 mab, respectively (Wilcoxon signed-rank test, $p < 0.05$), while there were no differences in C:N, C:P, and N:P ratios among depths (Fig. 5, Friedman test, all $p > 0.05$).

3.3. Grazing rates of lake seston

Depth-interval grazing rates (G) of lake seston varied substantially among trials (Fig. 6), with no significant differences among depths observed (Friedman test, all $p > 0.05$). Both negative grazing rates (i.e., seston concentration at effluence stations > affluence stations) and positive grazing rates (i.e., effluence < affluence) were tested (see Table S1 for detailed values, supporting information), and the highest grazing rates occurred at 0.25 or 0.5 mab (Fig. 6). At the 0.1 mab depth, average

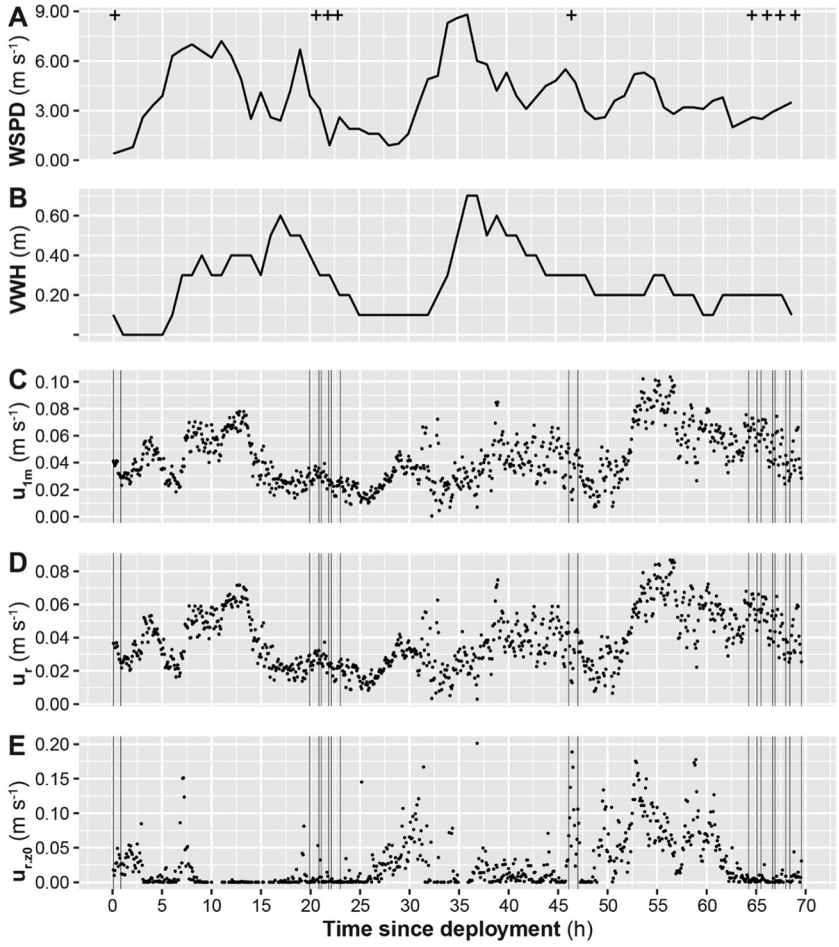

Fig. 2. Time series of (A) wind speed (WSPD), (B) vertical wave height (VWH), (C) flow velocity at one mab (u_{1m}), (D) depth-average flow velocity (u_r), and (D) flow velocity at 0.1 mab ($u_{r.z0}$) at the study site, and definitions of these variables are available in Table 1. Each pair of vertical lines (left to right) in C-E define a trial (i.e., beginning and end), corresponding to + symbols in A.

grazing rates were negative (Fig. 6A–E), leading to negative standardized scores across depths (i.e., negative Z scores in Fig. 6F). Within 0.1–0.5 mab, G.Chla (i.e., depth-interval grazing rate for Chla) displayed a significantly positive relationship with G.Phaeo ($r = 0.68$, $p < 0.0001$), and G.PON and G.POC were also correlated ($r = 0.54$, $p < 0.001$), but no other pairs were significantly correlated (Table S2, supporting information). Over the entire water column, depth-integrated grazing rates (G_{intg}; i.e., calculated from lake bottom upwards to the depth of interest) were negative in most cases except for the integrated G.Chla within 0.5 mab and G.PP within 0.25–1.5 mab (Fig. 7).

3.4. Relationships between grazing rates and environmental factors

Within the 0.1–0.5 mab zone, multiple regression models performed well in relating depth-interval grazing rates to multiple environmental factors, explaining 31.2–61.3 % of deviance (Table 3). Specifically, water depth (vs. G.Chla), flow velocity at 1.0 mab (u_{1m}) (vs. G.POC and G.PP), Chla (vs. G.POC and G.PON), and Chla: Phaeo ratio (vs. G.Phaeo) all demonstrated positive effects on grazing rates, although the C: N ratio had inconsistent effects (i.e., negative on G.Chla and G.Phaeo but positive on G.POC and G.PON; Table 3).

3.5. Relationships between grazing rates and stoichiometric ratios

With respect to the stoichiometry of lake seston, the most apparent changes in the horizontal direction were observed near the lake bottom (Fig. 8), but no significant differences were found among depths owing to considerable inter-trial variation (Friedman test, all $p > 0.05$). However, we identified a total of eight significantly ($p < 0.05$) correlated pairs of grazing rates and changes in stoichiometric ratios of lake seston (Fig. 9, Table S2), of which ΔC: N, ΔC: P, ΔN: P, and ΔChla: Phaeo were positively correlated with grazing rates, while the ΔN: P was negatively related to G.PON (Fig. 9).

4. Discussion

In this study we used a control volume approach to estimate in situ razing rates on lake seston by quagga mussels in eastern Lake Erie, with a special focus on the influence of multiple regulatory factors including stoichiometry of lake seston. Our study revealed that changes in stoichiometric ratios of lake seston were closely related to grazing rates in the horizontal direction, despite considerable variation in grazing rates among trials. Grazing rates on lake seston estimated via the control volume approach agreed with the vertical distribution of lake seston in field surveys. In situ grazing rates were associated with flow conditions, vertical distance towards mussels, food quantity, and stoichiometric ratios (i.e., food quality). Varying grazing rates on different nutrients suggested selective grazing, implying broad ecological impacts on large lakes. To the best of our knowledge, this represents the first application of an in situ control volume approach (e.g., Genin et al., 2009) in estimating grazing rates and impacts of dreissenid mussels. Although other studies on seston depletion over lake bottom encrusted by dreissenid mussels have been conducted in Lake Erie (e.g., MacIsaac et al., 1999; Ackerman et al., 2001), the present

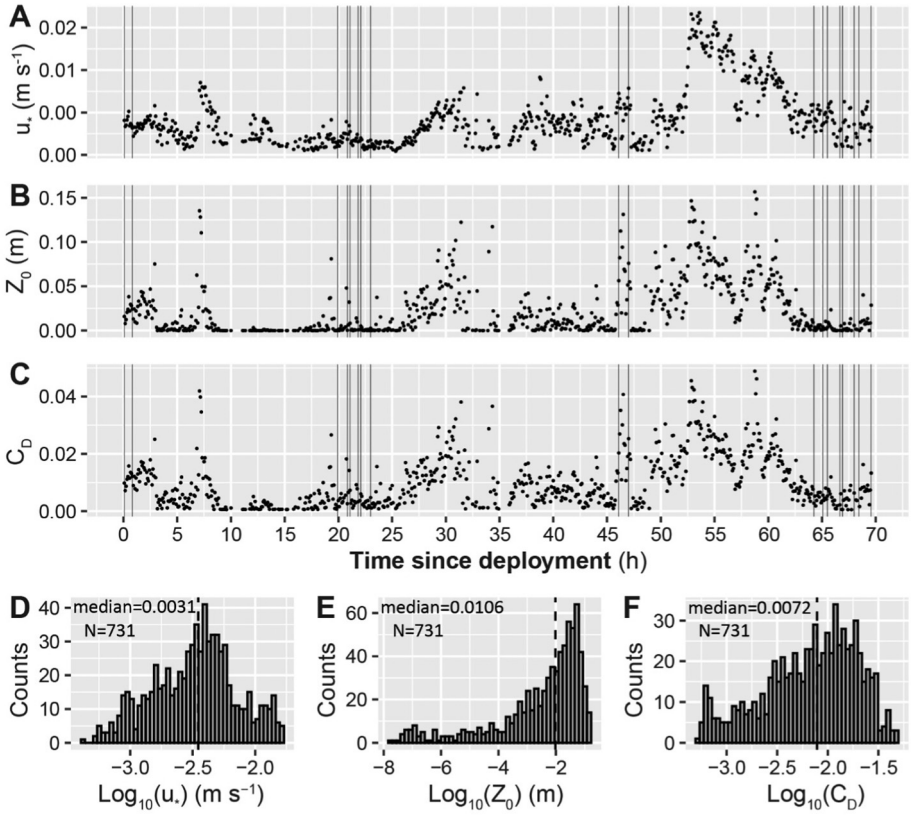

Fig. 3. Time series of (A) estimated shear velocity (u*), (B) roughness height (Z_0), and (C) drag coefficient (C_D) and their frequency distributions (D–F), respectively. Estimates of $u_* < 0$, $u_{r.z0} < 0$ and $u_{r.z0} > 1$, and $u_r < 0.01$ m s^{-1} are omitted in the plot. Each pair of vertical lines (left to right) in A-C define a trial, and vertical dashed lines in D–F represent median values.

study provides direct estimates of grazing rates of multiple lake seston-related parameters.

4.1. Physical conditions

Physical conditions such as thermal gradients and hydraulic mixing can affect grazing rates of many sessile species (Alpine and Cloern, 1992; MacIsaac et al., 1999; Ackerman et al., 2001; Wyatt et al., 2010; Xia et al., 2021). Water temperature during this study ranged between 24.4 and 26.7 °C, similar to previous surveys in summer in eastern Lake Erie (Depew et al., 2006), and fell within the optimal range of filtering activities of dreissenid mussels (MacIsaac, 1994; Diggins, 2001; Gopalakrishnan and Kashian, 2020; Xia et al., 2021). Temperature variation among depths never exceeded 1.7 °C, and no appreciable thermal stratification formed during our study (Fig. S1). These conditions were similar to previous nearshore surveys near our study site in eastern Lake Erie (e.g., Depew et al., 2006) and in the same season in the western basin of Lake Erie at comparable depths (MacIsaac, 1994; MacIsaac et al., 1999; Ackerman

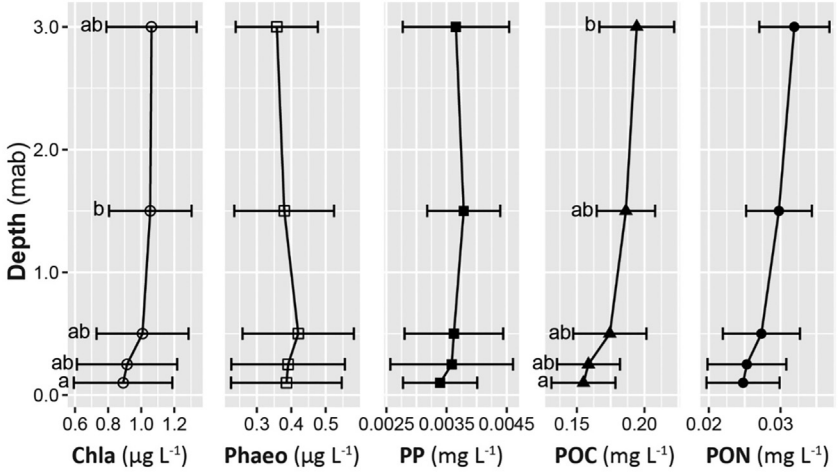

Fig. 4. Concentrations of lake seston (mean ± SD) at different depths above lake bottom. Different letters in panels Chla and POC indicate significant differences at $p = 0.05$ level (Wilcoxon signed-rank test) and those without letters indicate non-significance. Chla = chlorophyll *a*; Phaeo = pheaopigment; PP = particulate phosphorus; POC = particulate organic carbon; PON = particulate organic nitrogen.

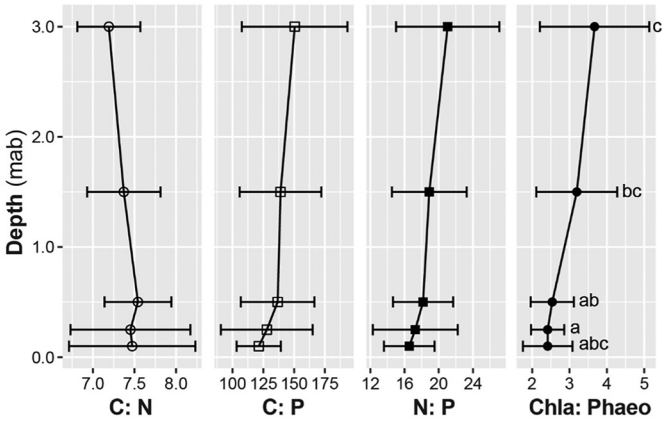

Fig. 5. Stoichiometries of lake seston (mean ± SD) at different depths within 0.1–3.0 mab zone. The Chla: Phaeo is mass ratio while the rest are molar ratios. Different letters in panel Chla: Phaeo indicate significant differences at $p = 0.05$ level (Wilcoxon signed-rank test) and those without letters indicate non-significance. C: N = molar POC: PON; C: P = molar POC: PP; N: P = molar PON: PP; Chla: Phaeo = mass Chla: Phaeo. See the Fig. 4 caption for lake seston codes.

et al., 2001). Such weak thermal stratification suggested that the vertical flux of lake seston to benthic communities was not limited by stratification; this might partially explain the weak depletion of lake seston within the 0.1–0.5 mab zone (Fig. 4), which was similar to observations in western Lake Erie under weak or unstratified conditions (e.g., MacIsaac et al., 1999; Ackerman et al., 2001).

Optimal flow velocities for grazing rates of quagga mussels are ~6–12 cm s^{-1} (Xia et al., 2021), which is ~2 to 4 times higher than the horizontal flow velocities we observed near the lake bottom ($u_{r.z0}$ = 2.8 cm s^{-1}). These observations were generally consistent with those reported previously for this nearshore region of the northeastern basin of Lake Erie (Leon et al., 2011; R.P. Weidman unpublished data, discussed in Xia et al., 2021), suggesting that mussels may have experienced suboptimal flow conditions. The significant positive correlation between u_{1m} and G.PP and G.POC (Table 3) also suggested that higher flow velocities increased grazing on PP and POC. Similar positive relationships between grazing rates and flow velocity are also reported for marine coral reefs (Genin et al., 2009).

Median shear velocity (u_*) in our study was ~0.3 cm s^{-1}, which was insufficient to completely mix the whole water column, according to Ackerman et al. (2001). Further, estimated average roughness height (Z_0) was ~1.1 cm, which was similar to previous estimates in the western basin of Lake Erie (~0.7 cm; MacIsaac et al., 1999) but lower than estimates obtained using a different method (i.e., 8–11 cm; Ackerman et al., 2001). At lake bottom, intensified mixing may have the dual effects of both resuspending sediment and enhancing grazing of lake seston by mussels (MacIsaac, 1994; Ackerman et al., 2001; Xia et al., 2021). In our study, shear velocity was negatively correlated to concentrations of all lake seston variables ($r = -0.58$ to -0.87, $p = 0.1028$–0.0023). This suggests that

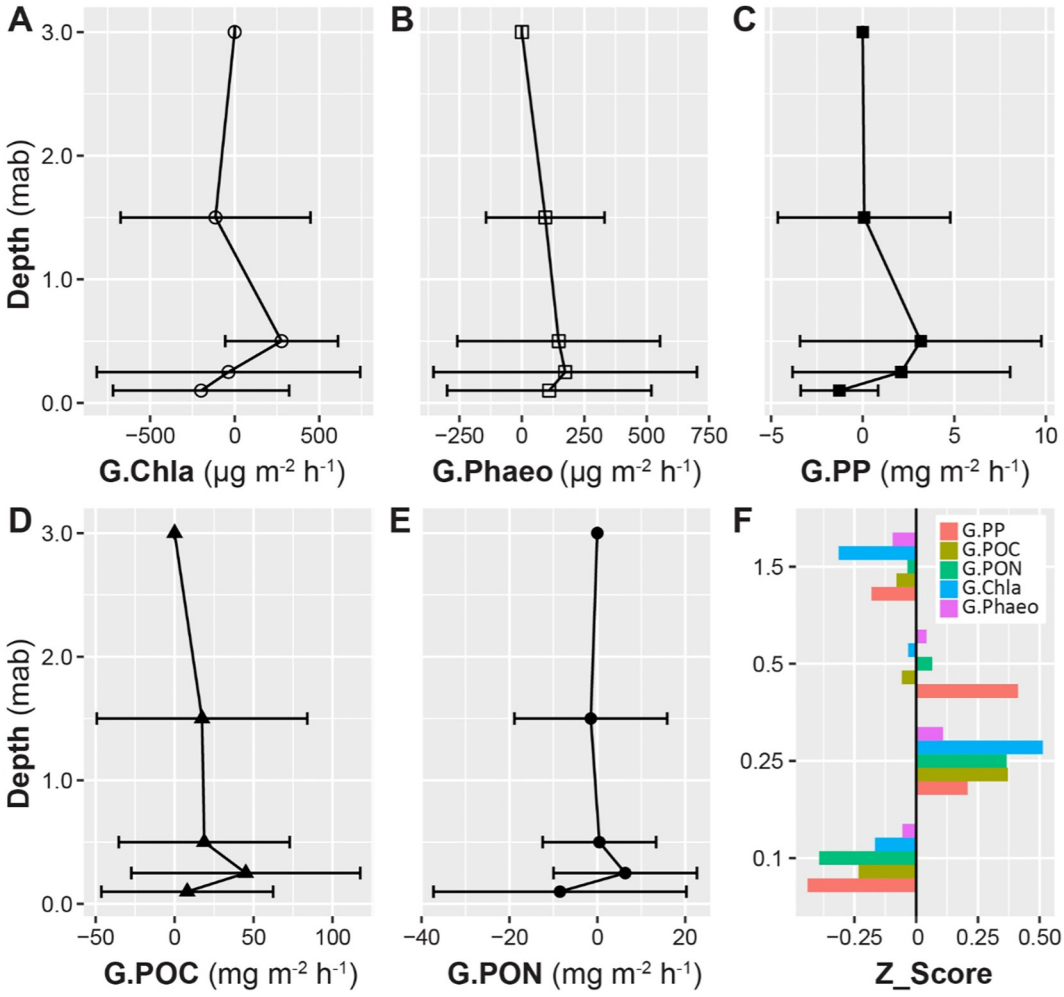

Fig. 6. Depth-interval grazing rates of lake seston (mean ± SD) (A–E) and their trial-averaged *Z*-transformed scores (F). A unit water column height of 1 m was used in calculating grazing rates. Grazing rates at 3.0 mab were zero because it was considered a control. Note the different y axis in F. See Fig. 4 for lake seston codes.

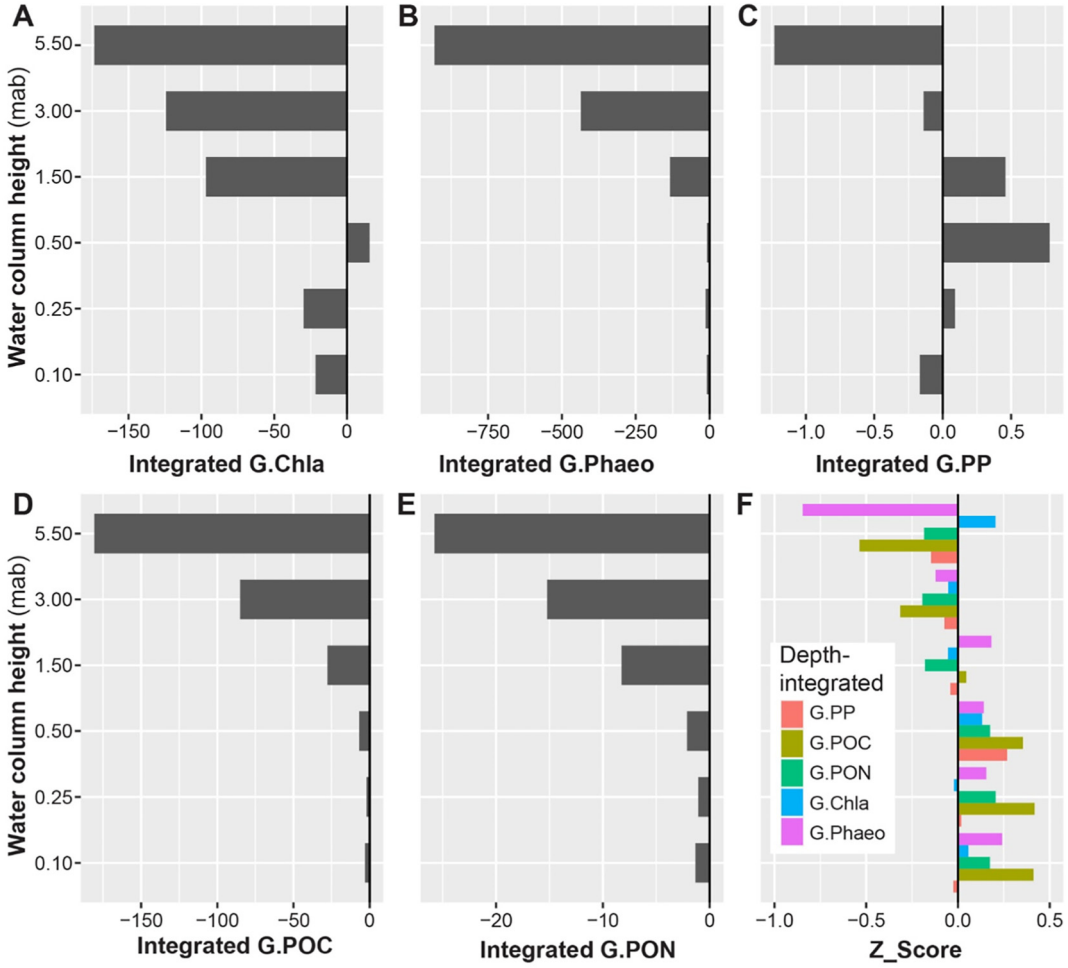

Fig. 7. Depth-integrated grazing rates of lake seston from the lake bottom to varying depths. Concentrations of lake seston at 3.0 mab were assigned to 5.5 mab for calculation. Standard deviations were omitted in plotting due to considerable variation (see results). See Fig. 4 for lake seston codes.

sediment resuspension at the lake bottom may be masked by mussel filtration, resulting in a net reduction of lake seston (Figs. 3 & 5). In addition, bottom shear stress can be estimated using $\tau = \rho \times C_D \times u_{1m}^2$ (Lorke and MacIntyre, 2009). Accordingly, median τ in our study was estimated as 1.13×10^{-2} N m^{-2} (estimated using median C_D). This was much lower than the critical shear stress measured in central Lake Erie (0.28 N m^{-2}) required to cause resuspension (Valipour et al., 2017). From linear wave theory, the observed peak wave period of 3.1 s is associated with a mean wave period of 2.2–2.6 s (Goda, 2000; Kamphuis, 2020). This value was lower than the theoretical value (2.8 s) allowing the wave-induced velocity to reach the bottom, which could be calculated according to the deep-water limit, i.e., depth > 0.5 wave length, and the dispersion relationship (Dean and Dalrymple, 1984; Goda, 2000). In addition, the study site is covered with bed rock and mussels, thus it is more resistant to the resuspension of bottom material compared to other parts of the lake as for example shown in Valipour et al. (2017).

Table 3
Summary of multiple linear regressions that relate net interval grazing rates of lake seston within the 0.1–0.5 mab zone to environmental factors. Significant variables at $p < 0.05$ are highlighted in bold.

	Model	Estimate	Std. error	t-value	*p*-value	AIC	Deviance explained
G.Chla	Intercept	14.1	97.4	0.15	0.8859	417.7	31.2 %
	Depth	214.3	99.4	2.16	**0.0414**		
	C: N	−259.3	99.4	−2.61	**0.0154**		
G.Phaeo	Intercept	143.4	54.1	2.65	0.0140	386.0	61.3 %
	C: N	−174.4	70	−2.49	**0.0200**		
	Chla: Phaeo	203.7	70	2.91	**0.0077**		
G.PP	Intercept	1.3	0.8	1.59	0.1260	161.8	42.7 %
	Depth	1.7	0.9	1.96	0.0625		
	C: N	1.4	0.9	1.48	0.1516		
	u_{1m}	3.4	0.9	3.60	**0.0015**		
G.POC	Intercept	23.9	8.4	2.85	0.0092	286.3	54.0 %
	Chla	30.0	8.9	3.38	**0.0026**		
	C: N	24.2	9.5	2.53	**0.0187**		
	u_{1m}	25.9	9.8	2.63	**0.0149**		
G.PON	Intercept	−0.6	3.3	−0.17	0.8662	234.9	40.9 %
	Chla	10.0	3.3	3.02	**0.0061**		
	C: N	8.0	4.2	2.39	**0.0255**		
	Chla: Phaeo	14.6	4.2	1.9	0.0697		

It was likely that mussels encountered food limitation on the lake bottom, even though vertical transport of lake seston from overlying water was not limited due to weak thermal stratification. Low absolute concentrations of lake seston (e.g., 0.1–0.2 mg POC L^{-1} and 0.4–1.4 μg Chla L^{-1}) would have limited optimal mussel grazing rates (Xia et al., 2021). We observed a depletion zone of seston within 0.1–0.5 mab (Fig. 4). This is consistent with a previous study in the western basin of Lake Erie where seston depletion was limited to <2.0 mab when mixing conditions were somewhat stronger than our study (u_* = 0.53 vs. 0.31 cm s^{-1}) (Ackerman et al., 2001). Dayton et al. (2014) found that a critical wave height of 0.2 m was sufficient to disrupt a concentration boundary layer of soluble reactive phosphorus at a site of 8 m deep in Lake Michigan. Given the shallower depth (6 vs. 8 m) and slightly more intensive waves (0.26 vs. 0.2 m) in our study, surface waves could have minimized formation of the weak depletion zone.

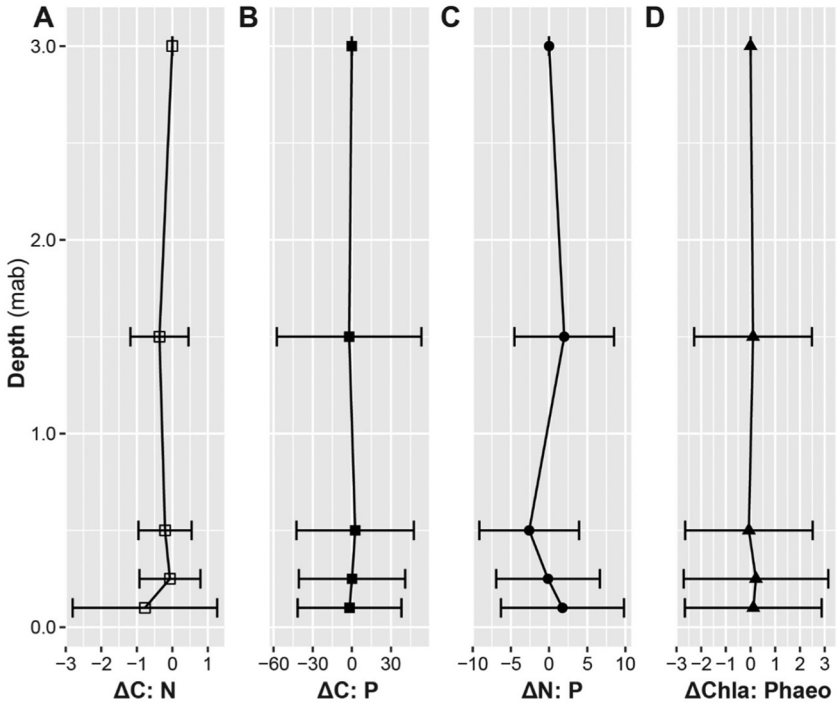

Fig. 8. Horizontal changes in stoichiometric ratios of lake seston (mean ± SD) at different depths above lake bottom. Values at 3.0 mab were zero because the layer was considered a control. No significant differences were detected among depths. See Fig. 5 for stoichiometric ratio codes.

Vertical profiles of lake seston combined with grazing rates estimated in the horizontal direction allowed us to define an effective grazing zone where the net removal of lake seston could be observed. The control volume approach revealed that despite considerable inter-trial variability the net effect of grazing by dreissenids was apparent at 0.25 and 0.50 mab (Fig. 6F). Given the lowest lake seston concentrations occurred at 0.1 mab, the effective grazing zone in our study ranged from 0.1 to 0.5 mab, within which the mussels appeared to deplete lake seston effectively (Figs. 4 & 6).

Grazing rates were lower at 0.1 mab relative to 0.25 and 0.5 mab (Fig. 6F), which suggested that complex mixing conditions at the lake bottom may have affected grazing. We also detected negative grazing rates above the effective grazing zone, which was likely a result of water mixing at the lake surface (MacIsaac et al., 1999) and relatively low mussel densities at our study site (4624 mussels per m^2) compared to other studies (e.g., 112,000–342,000 per m^2 in MacIsaac et al. (1999) and 7693 per m^2 in Ackerman et al., 2001). Differences in depth-integrated grazing rates between 0.1 and 0.5 mab and >1.5 mab (Fig. 7) indicate dominant role in concentration changes of lake seston near the bottom against natural processes such as sedimentation, which were more profound in the entire water column. Such spatial differences in impacts of dreissenids were consistent with other observations between nearshore and offshore regions of the Great Lakes. For example, nearshore reductions in seston concentrations were observed relative to offshore in eastern Lake Erie following the initial invasion of zebra mussels in the early 2000s (Hecky et al., 2004; North et al., 2012). However, complex conditions in nearshore regions such as inputs of seston from tributaries and wind-driven resuspension of seston in the nearshore can make the impact of grazing by dreissenids more apparent in offshore regions (e.g., Vanderploeg et al., 2010; Yurista et al., 2015; Pothoven and Vanderploeg, 2020).

Our estimation of grazing rates relied on measurable changes in lake seston concentration as water flowed along the lake bottom. Local mixing within the thin layer directly above the lake bottom (e.g., 0.1 mab) can be affected by several physical processes such as lakebed topology and shear stress (Ackerman et al., 2001), uneven 'hummock' distribution of mussels (MacIsaac et al., 1999), and mussel siphonal currents (Nishizaki and Ackerman, 2017). Further, even though water flow direction within trials was relatively consistent, it was observed to change among trials A–D, E–F, and G–I (Fig. 1). Weak correlations of flow condition variables between overlying water (i.e., u_r and u_{1m}) and near-bottom layers (i.e., $u_{r,z0}$; Table 2) suggested distinct hydrodynamic conditions at the lake bottom, which might have also contributed to the low grazing rates at 0.1 mab.

4.2. Food resources

Another important factor that affects grazing rates of bivalves is food concentration, which can have a positive effect on grazing rates, when food concentrations are low, before the mussels are satiated (Jeschke et al., 2004). Positive effects of increased food concentration have been found in many bivalves, such as the marine species *Mulinia edulis* and *Mytilus chilensis* (Bayne et al., 1993; Velasco and Navarro, 2002; Saurel et al., 2007) and freshwater species *Limnoperna fortunei* (Xia et al., 2020), *Dreissena polymorpha* (Sarnelle et al., 2015) and *D. rostriformis bugensis* (Xia et al., 2021). We found positive relationships between Chla and G. PON and G.POC (Table 3), which is consistent with a previous study on the same species collected from the same site (Xia et al., 2021). Indeed, Chla concentrations in this study were very low (0.4–1.4 μg L^{-1} at all sites), accounting for only ~5–10 % of that measured by Xia et al. (2021; 10.4–18.3 μg L^{-1}). Such low concentrations of Chla suggest that grazing rates of mussels could potentially increase in environments with higher seston concentrations because the filtering rate would remain high at low food concentrations (Jeschke et al., 2004; Sarnelle et al., 2015; Xia et al., 2020). In the western basin of Lake Erie, MacIsaac et al. (1999) and Ackerman et al. (2001) found that Chla concentration was depleted within 1.9 and 2.0 mab, respectively, but generally higher (1.1 to 5.0 μg L^{-1}) than our study. In addition, the present and previous studies were all conducted in May–October when Chla concentrations were the highest in Lake Erie (Depew et al., 2006; Chaffin et al., 2018), indicating that mussels may experience an extended period of food limitation in other months of the year. Body condition of zebra and quagga mussels (i.e., mass per unit length) decreases when they experience prolonged food shortage (Malkin et al., 2012; Vanderploeg et al., 2017). If this finding is applicable at broader scales, dreissenid mussels in deeper regions of the other Great

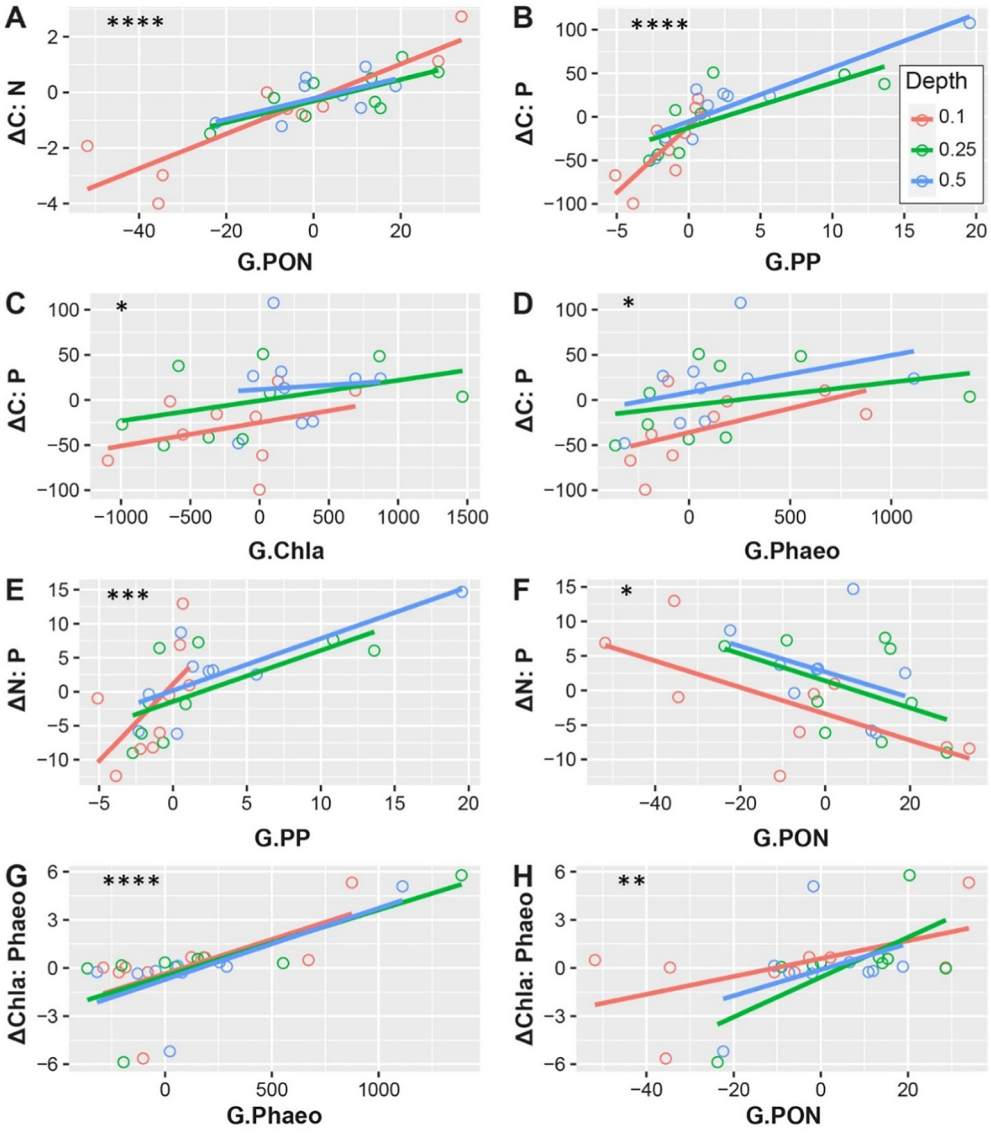

Fig. 9. Relationships between grazing rates and changes of stoichiometric ratios of lake seston within the 0.1–0.5 mab zone, showing significantly ($p = 0.05$) correlated pairs only. A regression line was added to each depth, while the significance level was examined based on pooled observations. Pearson correlation coefficients and significance levels for all pairs are available in Table S1. Units of grazing rates are available in Fig. 5. Significance level: * = 0.05, ** = 0.01, *** = 0.001, **** = 0.0001. See Fig. 4 for lake seston codes and Fig. 5 for stoichiometric ratio codes, respectively.

Lakes may be expected to suffer from long-term food limitation as well since these areas typically have lower primary productivity than Lake Erie (e.g., Vanderploeg et al., 2017; Rowland et al., 2020; Scofield et al., 2020).

Although Chla: Phaeo decreased towards the lake bottom - as we expected - owing to mussel grazing (Fig. 5), the horizontal change in this ratio (ΔChla: Phaeo) did not change with depth (Fig. 8). This finding suggested that local consumption of Chla by mussels might not be the major source of phaeopigment in our study (Monismith et al., 2010).

4.3. Grazing rates and seston stoichiometry

Previous studies have demonstrated that stoichiometric ratios of lake seston can influence grazing behavior and growth rate of bivalves via altered food quality (Velasco and Navarro, 2002; Vanderploeg et al., 2017). In our study, average ratios of C: P (138), N: P (19), and C: N (7; Table 1) in lake seston were somewhat higher than Redfield ratios (C:P = 106, N: P = 16; C:N = 7) but agree with observations in other Canadian lakes (Hecky et al., 1993; Naddafi et al., 2008). Seston N: P (mean: 19, range: 11–32) might indicate that N was slightly limiting for mussel growth because previous studies have found average zebra mussel tissue N: P ranged from 17 to 45 (Naddafi et al., 2008; Vanderploeg et al., 2017; Williamson and Ozersky, 2019). In contrast, we did not expect P to limit mussel growth because the C: P of lake seston (mean: 138, range: 83–229) was similar to average ratios (range: 91–155) found in zebra mussel tissues in the aforementioned studies. We could not find similar tissue data for quagga mussels in the literature, although we expect comparable stoichiometric ratios between the two species.

Unlike concentrations of lake seston which were positively related to each other (Table 2), grazing rates of lake seston were usually not related (except G.Chla vs. G.Phaeo, $r = 0.68$ and G.PON vs. G.POC, $r = 0.54$). Such observations might suggest selective grazing of dreissenid mussels on different nutrients. For example, C: N was negatively related to G.Chla and G.Phaeo (Table 3), which suggests that quagga mussels may have preferred phytoplankton with higher N content (i.e., higher food quality). While this possibility has been reported for zebra mussels (Vanderploeg et al., 2017), to our knowledge no similar data exists for quagga mussels.

In contrast, C: N was positively related to G.PON and G.POC (Table 3), which suggests food limitation because of the low absolute POC concentration (0.2 mg L^{-1}) and the positive relationship between POC and PON (Table 2). The positive correlation between ΔChla: Phaeo and G.Phaeo (Fig. 9) indicates that mussel ingestion or re-ingestion of dead algae may have occurred, while further research is required. Selective ejection/rejection of food materials by dreissenids may have profound impacts on ecosystems. For example, zebra mussels can alter phytoplankton community composition through selective rejection of toxic *Microcystis aeruginosa* (Vanderploeg et al., 2001) or change soluble nutrient ratios under different feeding conditions via selective excretion (Bykova et al., 2006; Vanderploeg et al., 2017).

Mussel grazing impacted changes in stoichiometric ratios of lake seston as predicted by ecological stoichiometry theory (Elser et al., 2000; Frost et al., 2002). More consistent correlations were found between grazing rates and changes in seston stoichiometric ratios (Fig. 9; Table S3, supporting information) versus correlations with absolute ratios. Specifically, (1) grazing on N led to increased ΔC: N and decreased ΔN: P; (2) grazing on P resulted in increased ΔN: P and ΔC: P; (3) grazing on Phaeo increased ΔChla: Phaeo; and (4) grazing on Chla and Phaeo (i.e., living and dead phytoplankton components of seston, respectively) increased ΔC: P, suggesting net retention of P by mussels. Thus, despite substantial natural variation in absolute stoichiometric ratios of lake seston near the lake bottom, such variations were minimized by analyzing their changes following water flow over mussel reefs. This revealed significant effects of mussel grazing on nutrient composition of lake seston. Observed correlations between changes in stoichiometric ratios and grazing rates were also consistent with vertical patterns of stoichiometric ratios of lake seston within the effective grazing zone (0.1–0.5 mab; Figs. 4–7).

Grazing on PP (G.PP) had a stronger effect than G.PON on ΔN: P when the two covariates were compared simultaneously in the same linear model, which yielded a greater absolute standardized coefficient for G.PP than G.PON (i.e., 0.76 vs. −0.62; data not shown). This suggests that on a molar basis, overall grazing rates were greater for PP than for PON, which in turn was greater than for POC. These findings were consistent with other studies of zebra mussels, which had stronger effects on C:P and N:P than C:N (Naddafi et al., 2008). Similarly, zebra mussel excretion is higher for nitrate than phosphate in microcosm sediments (Bykova et al., 2006). These findings are consistent with the nearshore P shunt hypothesis that P is preferentially retained in nearshore regions following the establishment of dreissenids (Hecky et al., 2004).

The above findings suggest ecologically important associations exist between mussel grazing activities and stoichiometric ratios of lake seston. Disproportionate grazing on key nutrients in lake seston has profound ecological implications for driving stoichiometric imbalances between producers and consumers (Elser et al., 2000; Frost et al., 2002), potentially at large temporal and spatial scales in Great Lakes ecosystems. For example, faster grazing rates of PP than PON suggest that P may be differentially redirected to the benthos by dreissenids. Enrichment of P near the lake bottom by quagga mussels, together with their rapid expansion to greater depths, have made this species a predominant player in P cycling in the Great Lakes (Li et al., 2021). However, differential consumption and excretion of C, N, and P by dreissenid mussels may depend on season, food quality, and mussel size (Vanderploeg et al., 2017; Williamson and Ozersky, 2019). Despite fewer studies, it is reasonable to expect that homeostatic control in quagga mussels might also lead to selective grazing on lake seston, as has been reported for zebra mussels (Vanderploeg et al., 2017). Future in situ studies that investigate stoichiometric changes of lake seston and soluble nutrients may further advance our understanding of these issues.

4.4. Considerations for the control volume approach

One potential source of error in our estimation of depth-interval grazing rates lies in the absence of true experimental control trials using the exact same experimental settings but without mussels. A possible control treatment could involve the deployment of plastic sheets that cover the mussel bed, allowing assessments above the plastic sheets to represent mussel-free conditions (e.g., Genin et al., 2009). Although we attempted such controls, our study area proved too large for this approach. Another solution could be to conduct similar deployments at nearby sites that lacked mussels. With either of these potential control treatments, however, differences in hydraulic conditions along the lake bottom would have to be considered.

We considered the 3.0 mab layer as a simplified control to correct our estimations for sedimentation of seston, which should allow for more accurate estimates of natural grazing rates within the effective grazing zone (0.1–0.5 mab). However, this procedure may not fully control the effects of natural sedimentation because of the different hydrodynamic conditions, such as flow velocity and wave influence at 3.0 mab compared to the lake bottom. In addition, we calculated depth-interval grazing rates (G) without considering potential vertical flux of seston within the simplified 1 m depth intervals, which could have resulted in another source of error. Overall, depth-integrated grazing rates were negative when the entire water column was considered, while positive rates were obtained if only the near-bottom layers were considered (Fig. S3). This disparity is consistent with the observed differences between depth-interval grazing rates (Fig. 6; Table S1), further supporting that direct grazing of lake seston was restricted to near the lake bottom.

A critical assumption of the control volume approach is that flow direction and velocity are consistent between sampling stations (Wyatt et al., 2010). In our study, flow direction varied among trials (Fig. 1) even though it was relatively consistent within each trial. To what extent the changes of flow direction can affect the advection of lake seston and their impacts on subsequent trials requires more research.

One other source of uncertainty stems from the scale of the control volume. Our study system was comparable in size to that of studies in marine ecosystems (e.g., Genin et al., 2009; Monismith et al., 2010). A larger control volume may allow for greater lake seston concentration changes along the lake bottom, however, it may also introduce more variation with respect to the topography of the lake bottom, patchy distribution of mussels, and flow divergence between sampling stations (MacIsaac et al., 1999; Genin et al., 2009; Wyatt et al., 2010). Effects of these factors may diminish under uniform flow conditions such as consistent flow direction with suitable velocity, but these conditions are unrealistic to obtain in nearshore regions of large lakes. Future applications of the control volume approach should be conducted where more dense mussels are present to maximize lake seston depletion and more consistent flow conditions occur to reduce natural variation.

5. Conclusions

Invasive dreissenid mussels play a critical role in redirecting nutrient fluxes in invaded ecosystems, which in turn are regulated by multiple environmental factors such as flow conditions, food supply and quality. We found that when the water column was unstratified, direct effects of grazing on lake seston by quagga mussels were only apparent within a shallow zone below 0.5 mab. Net grazing on lake seston was hard to detect within the entire water column, but it was detected at discrete depths near the lake bottom. Within the effective grazing zone, grazing rates calculated in the horizontal direction were consistent with changes in the vertical distribution of lake seston, except in the layer immediately above lake bottom (0.1 mab). Consistent with laboratory studies, grazing rates were significantly related to flow velocity, water depth, and seston concentrations. Changes in stoichiometric ratios of lake seston were also closely related to grazing rates within the effective grazing zone, which suggested selective grazing by quagga mussels on P. Specifically, greater grazing rates on PP than PON and POC suggested that more PP was redirected to the benthos, providing direct evidence in support of the nearshore P shunt hypothesis. Our findings imply profound impacts of invasive dreissenids on nutrient cycling and strong influences of environmental factors on these processes.

Author contributions

ZX led the study, statistical analysis, and writing of the manuscript. DCD and RV conducted the experiments and collected the data. RPW provided conceptualization and supervision. All authors contributed to writing and revising the manuscript and approved the final version.

Data accessibility

Supporting information can be found online for this paper.

Data availability

Data will be made available on request.

Declaration of competing interest

The authors declare that they have no known competing financial interests or personal relationships that could have appeared to influence the work reported in this paper.

Acknowledgments

We dedicate this paper to the memory of our friend and late colleague, Dr. William (Bill) D. Taylor, for his indomitable and kind spirit and tremendous scientific contributions to freshwater ecology and the understanding of phosphorus cycling in large lakes in North America, Africa, and China. We are grateful for the insightful comments by two anonymous referees.

Field and laboratory support was provided by staff at Environment & Climate Change Canada, Watershed Hydrology & Ecology Research Division. Funding was provided by an NSERC Discovery Grant and Canada Research Chair in Aquatic Invasive Species (HJM) and by the Great Lakes Nutrient Initiative of Environment & Climate Change Canada (RPW).

Appendix A. Supplementary data

Supplementary data to this article can be found online at https://doi.org/10.1016/j.scitotenv.2022.157924.

References

Ackerman, J.D., Loewen, M.R., Hamblin, P.F., 2001. Benthic-pelagic coupling over a zebra mussel reef in western Lake Erie. Limnol. Oceanogr. 46, 892–904.

Alpine, A.E., Cloern, J.E., 1992. Trophic interactions and direct physical effects control phytoplankton biomass and production in an estuary. Limnol. Oceanogr. 37, 946–955.

Bayne, B.L., Iglesias, J.I.P., Hawkins, A.J.S., Navarro, E., Heral, M., Deslous-Paoli, J.M., 1993. Feeding behaviour of the mussel, Mytilus edulis: responses to variations in quantity and organic content of the seston. J. Mar. Biol. Assoc. U. K. 73, 813–829.

Benelli, S., Bartoli, M., Zilius, M., Vybernaite-Lubiene, I., Ruginis, T., Vaiciute, D., Petkuviene, J., Fano, E., 2019. Stoichiometry of regenerated nutrients differs between native and invasive freshwater mussels with implications for algal growth. Freshw. Biol. 64, 619–631. https://doi.org/10.1111/fwb.13247.

Boegman, L., Lowewen, M.R., Hamblin, P.F., Culver, D.A., 2008. Vertical mixing and weak stratification over zebra mussel colonies in western Lake Erie. Limnol. Oceanogr. 53, 1093–1110.

Burlakova, L.E., Karatayev, A.Y., Hrycik, A.R., Daniel, S.E., Mehler, K., Rudstam, L.G., Nalepa, T.F., 2021. Six decades of Lake Ontario ecological history according to benthos. J. Great Lakes Res. https://doi.org/10.1016/j.jglr.2021.03.006.

Bykova, O., Laursen, A., Bostan, V., Bautista, J., McCarthy, L., 2006. Do zebra mussels (Dreissena polymorpha) alter lake water chemistry in a way that favours microcystis growth? Sci. Total Environ. 371, 362–372. https://doi.org/10.1016/j.scitotenv.2006.08.022.

Chaffin, J.D., Kane, D.D., Stanislawczyk, K., Parker, E.M., 2018. Accuracy of data buoys for measurement of cyanobacteria, chlorophyll, and turbidity in a large lake (Lake Erie, North America): implications for estimation of cyanobacterial bloom parameters from water quality sonde measurements. Environ. Sci. Pollut. Res. 25, 25175–25189.

Connelly, N.A., O'Neill Jr., C.R., Knuth, B.A., Brown, T.L., 2007. Economic impacts of zebra mussels on drinking water treatment and electric power generation facilities. Environ. Manag. 40, 105–112. https://doi.org/10.1007/s00267-006-0296-5.

Conroy, J.D., Edwards, W.J., Pontius, R.A., Kane, D.D., Zhang, H., Shea, J.F., Richey, J.N., Culver, D.A., 2005. Soluble nitrogen and phosphorus excretion of exotic freshwater mussels (Dreissena spp.): potential impacts for nutrient remineralization in western Lake Erie. Freshw. Biol. 50, 1146–1162. https://doi.org/10.1111/j.1365-2427.2005.01392.x.

Coughlan, J., 1969. The estimation of filtering rate from the clearance of suspensions. Mar. Biol. 2, 356–358.

Dayton, A.I., Auer, M.T., Atkinson, J.F., 2014. Cladophora, mass transport, and the nearshore phosphorus shunt. J. Great Lakes Res. 40, 790–799. https://doi.org/10.1016/j.jglr.2014.05.010.

Dean, R.G., Dalrymple, R.A., 1984. Water wave mechanics for engineers and scientists. Adv. Ser. Ocean Eng. https://doi.org/10.1142/9789812385512.

Depew, D.C., Guildford, S.J., Smith, R.E.H., 2006. Nearshore-offshore comparison of chlorophyll a and phytoplankton production in the dreissenid-colonized eastern basin of Lake Erie. Can. J. Fish. Aquat. Sci. 63, 1115–1129. https://doi.org/10.1139/F06-016.

Diggins, T.P., 2001. A seasonal comparison of suspended sediment filtration by quagga (Dreissena bugensis) and zebra (D. polymorpha) mussels. J. Great Lakes Res. 27, 457–466. https://doi.org/10.1016/S0380-1330(01)70660-0.

Elser, J.J., Fagan, W.F., Denno, R.F., Dobberfuhl, D.R., Folarin, A., Huberty, A., Sterner, R.W., 2000. Nutritional constraints in terrestrial and freshwater food webs. Nature 408, 578–580. https://doi.org/10.1038/35046058.

Fera, S.A., Rennie, M.D., Dunlop, E.S., 2017. Broad shifts in the resource use of a commercially harvested fish following the invasion of dreissenid mussels. Ecology 98, 1681–1692.

Fox, J., Weisberg, S., 2019. An {R} Companion to Applied Regression. URL:Third edition. Sage, Thousand Oaks CA. https://socialsciences.mcmaster.ca/jfox/Books/Companion/.

Frost, P.C., Stelzer, R.S., Lamberti, G.A., Elser, J.J., 2002. Ecological stoichiometry of trophic interactions in the benthos: understanding the role of C:N: P ratios in lentic and lotic habitats. J. N. Am. Benthol. Soc. 21, 515–528.

Genin, A., Monismith, S.G., Reidenbach, M.A., Yahel, G., Koseff, J.R., 2009. Intense benthic grazing of phytoplankton in a coral reef. Limnol. Oceanogr. 54, 938–951.

Gergs, R., Rothhaupt, K.-O., 2008. Feeding rates, assimilation efficiencies and growth of two amphipod species on biodeposited material from zebra mussels. Freshw. Biol. 53, 2494–2503. https://doi.org/10.1111/j.1365-2427.2008.02077.x.

Goda, Y., 2000. Random Seas And Design Of Maritime Structures. 2nd edition. World Scientific Publishing Company.

Gopalakrishnan, K.K., Kashian, D.R., 2020. Identification of optimal calcium and temperature conditions for quagga mussel filtration rates as a potential predictor of invasion. Environ. Toxicol. Chem. 39, 410–418. https://doi.org/10.1002/etc.4624.

Heath, R.T., Fahnenstiel, G.L., Gardner, W.S., Cavaletto, J.F., Hwang, S.-J., 1995. Ecosystem-level effects of zebra mussels (Dreissena polymorpha): an enclosure experiment in Saginaw Bay, Lake Huron. J. Great Lakes Res. 21, 501–516.

Hecky, R.E., Campbell, P., Hendzel, L.L., 1993. The stoichiometry of carbon, nitrogen, and phosphorus in particulate matter of lakes and oceans. Limnol. Oceanogr. 38, 709–724.

Hecky, R.E., Smith, R.E.H., Barton, D.R., Guildford, S.J., Taylor, W.D., Charlton, M.N., Howell, T., 2004. The nearshore phosphorus shunt: a consequence of ecosystem engineering by dreissenids in the laurentian Great Lakes. Can. J. Fish. Aquat. Sci. 61, 1285–1293. https://doi.org/10.1139/F04-065.

Higgins, S.N., Vander Zanden, M.J., 2010. What a difference a species makes: a meta-analysis of dreissenid mussels impacts on freshwater ecosystems. Ecol. Monogr. 80, 179–196. https://doi.org/10.1890/09-1249.1.

Higgins, S.N., Hecky, R.E., Guildford, S.J., 2006. Environmental controls of cladophora growth dynamics in eastern Lake Erie: application of the cladophora growth model (CGM). J. Great Lakes Res. 32, 629–644. https://doi.org/10.3394/0380-1330(2006)32[629:ECOCGD]2.0.CO;2.

Jabbari, A., Ackerman, J.D., Boegman, L., Zhao, Y., 2021. Increases in Great Lakes winds and extreme events facilitate interbasin coupling and reduce water quality in Lake Erie. Sci. Rep. 11, 5733. https://doi.org/10.1038/s41598-021-84961-9.

Jeschke, J.M., Kopp, M., Tollrian, R., 2004. Consumer-food systems: why type I functional responses are exclusive to filter feeders. Biol. Rev. 79, 337–349. https://doi.org/10.1017/S1464793103006286.

Jørgensen, C.B., Larsen, P.S., Riisgård, H.G., 1990. Effects of temperature on the mussel pump. Mar. Ecol. Prog. Ser. 64, 89–97.

Kamphuis, J.W., 2020. Introduction To Coastal Engineering And Management. 3rd edition. World Scientific.

Karatayev, A.Y., Karateyev, V.A., Burlakova, L.E., Mehler, K., Rowe, M.D., Elgin, A.K., Nalepa, T.F., 2021. Lake morphometry determines dreissena invasion dynamics. Biol. Invasions https://doi.org/10.1007/s10530-021-02518-3.

Karatayev, A.Y., Burlakova, L.E., Mehler, K., Elgin, A.K., Rudstam, L.G., Watkins, J.M., Wick, M., 2022. Dreissena in Lake Ontario 30 years post-invasion. J. Great Lakes Res. 48, 264–273. https://doi.org/10.1016/j.jglr.2020.11.010.

Kassambara, A., 2021. rstatix: pipe-friendly framework for basic statistical tests. R package version 0.7.0. https://CRAN.R-project.org/package=rstatix.

Leon, L.F., Smith, R.E.H., Hipsey, M.R., Bocaniov, S.A., Higgins, S.N., Hecky, R.E., Guildford, S.J., 2011. Application of a 3D hydrodynamic-biological model for seasonal and spatial dynamics of water quality and phytoplankton in Lake Erie. J. Great Lakes Res. 37, 41–53. https://doi.org/10.1016/j.jglr.2010.12.007.

Li, J., Ianaiev, V., Huff, A., Zalusky, J., Ozersky, T., Katsev, S., 2021. Benthic invaders control the phosphorus cycle in the world's largest freshwater ecosystem. Proc. Natl. Acad. Sci., 118 https://doi.org/10.1073/pnas.2008223118.

Lorke, A., MacIntyre, S., 2009. The benthic boundary layer (in Rivers, Lakes, and Reservoirs). In: Likens, G.E. (Ed.), Encyclopedia of Inland Waters. Academic Press, pp. 505–514 https://doi.org/10.1016/B978-012370626-3.00079-X.

Lorke, A., Umlauf, L., Jonas, T., Wüest, A., 2002. Dynamics of turbulence in low-speed oscillating bottom-boundary layers of stratified basins. Environ. Fluid Mech. 2, 291–313.

MacIsaac, H.J., 1994. Comparative growth and survival of Dreissena polymorpha and Dreissena bugensis, exotic molluscs introduced to the Great Lakes. J. Great Lakes Res. 20, 783–790.

MacIsaac, H.J., 1996. Potential abiotic and biotic impacts of zebra mussels on the inland waters of North America. Am. Zool. 36, 287–299.

MacIsaac, H.J., Sprules, W.G., Johannsson, O.E., Leach, J.H., 1992. Filtering impacts of larval and sessile zebra mussels (Dreissena polymorpha) in western Lake Erie. Oecologia 92, 30–39.

MacIsaac, H.J., Johannsson, O.E., Ye, J., Sprules, W.G., Leach, J.H., McCorquodale, J.A., Grigorovich, I.A., 1999. Filtering impacts of an introduced bivalve (Dreissena polymorpha) in a shallow lake: application of a hydrodynamic model. Ecosystems 2, 338–350.

Malkin, S.Y., Silsbe, G.M., Smith, R.E.H., Howell, E.T., 2012. A deep chlorophyll maximum nourishes benthic filter feeders in the coastal zone of a large clear lake. Limnol. Oceanogr. 57, 735–748. https://doi.org/10.4319/lo.2012.57.3.0735.

Monismith, S.G., Davis, K.A., Shellenbarger, G.G., Hench, J.L., Nidzieko, N.J., Santoro, A.E., Geninf, A., 2010. Flow effects on benthic grazing on phytoplankton by a Caribbean reef. Limnol. Oceanogr. 55, 1881–1892. https://doi.org/10.4319/lo.2010.55.5.1881.

Mosley, M., Bootsma, H., 2015. Phosphorus recycling by profunda quagga mussels (Dreissena rostriformis bugensis) in Lake Michigan. J. Great Lakes Res. 41 (Supplement 3), 38–48.

Naddafi, R., Pettersson, K., Eklöv, P., 2007. The effect of seasonal variation in selective feeding by zebra mussels (Dreissena polymorpha) on phytoplankton community composition. Freshw. Biol. 52, 823–842. https://doi.org/10.1111/j.1365-2427.2007.01732.x.

Naddafi, R., Pettersson, K., Eklöv, P., 2008. Effects of the zebra mussel, an exotic freshwater species, on seston stoichiometry. Limnol. Oceanogr. 53, 1973–1987.

Nishizaki, M., Ackerman, J.D., 2017. Mussel blow rings: jet behavior affects local mixing. Limnol. Oceanogr. 62, 125–136. https://doi.org/10.1002/lno.10380.

North, R.L., Smith, R.E.H., Hecky, R.E., Depew, D.C., León, L.F., Charlton, M.N., Guildford, S.J., 2012. Distribution of seston and nutrient concentrations in the eastern basin of Lake Erie pre- and post-dreissenid mussel invasion. J. Great Lakes Res. 38, 463–476.

Ozersky, T., Evans, D.O., Ginn, B.K., 2015. Invasive mussels modify the cycling, storage and distribution of nutrients and carbon in a large lake. Freshw. Biol. 60, 827–843. https://doi.org/10.1111/fwb.12537.

Pinheiro, J., Bates, D., DebRoy, S., Sarkar, D.R., Core Team, 2021. nlme: Linear and Nonlinear Mixed Effects Models. R Package Version 3.1-153.

Pothoven, S.A., Vanderploeg, H.A., 2020. Seasonal patterns for secchi depth, chlorophyll a, total phosphorus, and nutrient limitation differ between nearshore and offshore in Lake Michigan. J. Great Lakes Res. 46, 519–527. https://doi.org/10.1016/j.jglr.2020.03.013.

R Core Team, 2020. R: a language and environment for statistical computing. R Foundation for Statistical Computing, Vienna, Austria. https://www.R-project.org/.

Rowland, F.E., Stow, C.A., Johengen, T.H., Burtner, A.M., Palladino, D., Gossiaux, D.C., Ruberg, S., 2020. Recent patterns in Lake Erie phosphorus and chlorophyll a concentrations in response to changing loads. Environ. Sci. Technol. 54, 835–841.

Sarnelle, O., White, J.D., Geelhoed, T.E., Kozel, C., 2015. Type III functional response in the zebra mussel, Dreissena polymorpha. Can. J. Fish. Aquat. Sci. 72, 1202–1207. https://doi.org/10.1139/cjfas-2015-0076.

Saurel, C., Gascoigne, J.C., Palmer, M.R., Kaiser, M.J., 2007. In situ mussel feeding behavior in relation to multiple environmental factors: regulation through food concentration and tidal conditions. Limnol. Oceanogr. 52, 1919–1929.

Scofield, A.E., Watkins, J.M., Osantowski, E., Rudstam, L.G., 2020. Deep chlorophyll maxima across a trophic state gradient: a case study in the laurentian Great Lakes. Limnol. Oceanogr. 65, 2460–2484.

Shen, C., Liao, Q., Bootsma, H.A., 2020. Modelling the influence of invasive mussels on phosphorus cycling in Lake Michigan. Ecol. Model. 416, 108920. https://doi.org/10.1016/j.ecolmodel.2019.108920.

Sterner, R.W., 2021. The laurentian Great Lakes: a biogeochemical test bed. Annu. Rev. Earth Planet. Sci. 49. https://doi.org/10.1146/annurev-earth-071420-051746.

Sterner, R.W., Ostrom, P., Ostrom, N.E., Klump, J.V., Steinman, A.D., Dreelin, E.A., Fisk, A.T., 2017. Grand challenges for research in the laurentian Great Lakes. Limnol. Oceanogr. 62, 2510–2523. https://doi.org/10.1002/lno.10585.

Strayer, D.L., 2009. Twenty years of zebra mussels: lessons from the mollusk that made headlines. Front. Ecol. Environ. 7, 135–141. https://doi.org/10.1890/080020.

Valipour, R., Bouffard, D., Boegman, L., 2015. Parameterization of bottom mixed layer and logarithmic layer heights in Central Lake Erie. J. Great Lakes Res. 41, 707–7018. https://doi.org/10.1016/j.jglr.2015.06.010.

Valipour, R., Boegman, L., Bouffard, D., Rao, Y.R., 2017. Sediment resuspension mechanisms and their contributions to high-turbidity events in a large lake. Limnol. Oceanogr. 62, 1045–1065. https://doi.org/10.1002/lno.10485.

Valipour, R., Rao, Y.R., León, L.F., Depew, D., 2019. Nearshore-offshore exchanges in multi-basin coastal waters: observations and three-dimensional modelling in Lake Erie. J. Great Lakes Res. 45, 50–60. https://doi.org/10.1016/j.jglr.2018.10.005.

Vanderploeg, H.A., Liebig, J.R., Carmichael, W.W., Agy, M.A., Johengen, T.H., Fahnenstiel, G.L., Nalepa, T.F., 2001. Zebra mussel (Dreissena polymorpha) selective filtration promoted toxic microcystis blooms in Saginaw Bay (Lake Huron) and Lake Erie. Can. J. Fish. Aquat. Sci. 58, 1208–1221. https://doi.org/10.1139/cjfas-58-6-1208.

Vanderploeg, H.A., Liebig, J.R., Nalepa, T.F., Fahnenstiel, G.L., Pothoven, S.A., 2010. Dreissena and the disappearance of the spring phytoplankton bloom in Lake Michigan. J. Great Lakes Res. 36 (Suppl. 3), 50–59. https://doi.org/10.1016/j.jglr.2010.04.005.

Vanderploeg, H.A., Sarnelle, O., Liebig, J.R., Morehead, N.R., Robinson, S.D., Johengen, T.H., Horst, G.P., 2017. Seston quality drives feeding, stoichiometry and excretion of zebra mussels. Freshw. Biol. 62, 664–680.

Velasco, L.A., Navarro, J.M., 2002. Feeding physiology of infaunal (Mulinia edulis) and epifaunal (Mytilus chilensis) bivalves under a wide range of concentrations and qualities of seston. Mar. Ecol. Prog. Ser. 240, 143–155.

Watson, S.B., Miller, C., Arhonditsis, G., Boyer, G.L., Carmichael, W., Charlton, M.N., Wilhelm, S.W., 2016. The re-eutrophication of Lake Erie: harmful algal blooms and hypoxia. Harmful Algae 56, 44–66.

Williamson, F., Ozersky, T., 2019. Lake characteristics, population properties and invasion history determine impact of invasive bivalves on lake nutrient dynamics. Ecosystems 22, 1721–1735. https://doi.org/10.1007/s10021-019-00371-z.

Wyatt, A.S.J., Lowe, R.J., Humphries, S., Waite, A.M., 2010. Particulate nutrient fluxes over a fringing coral reef: relevant scales of phytoplankton production and mechanisms of supply. Mar. Ecol. Prog. Ser. 405, 113–130. https://doi.org/10.3354/meps08508.

Xia, Z., Cao, X., Hoxha, T., Zhan, A., Haffner, G.D., MacIsaac, H.J., 2020. Functional response and size-selective clearance of suspended matter by an invasive mussel. Sci. Total Environ. 711, 134679. https://doi.org/10.1016/j.scitotenv.2019.134679.

Xia, Z., MacIsaac, H.J., Hecky, R.E., Depew, D.C., Haffner, G.D., Weidman, R.P., 2021. Multiple factors regulate filtration by invasive mussels: implications for whole-lake ecosystems. Sci. Total Environ. 765, 144435. https://doi.org/10.1016/j.scitotenv.2020.144435.

Yurista, P.M., Kelly, J.R., Cotter, A.M., Miller, S.E., Van Alstine, J.D., 2015. Lake Michigan: nearshore variability and a nearshore-offshore distinction in water quality. J. Great Lakes Res. 41, 111–122. https://doi.org/10.1016/j.jglr.2014.12.010.

Zuur, A., Ieno, E.N., Walker, N., Saveliev, A.A., Smith, G.M., 2009. Mixed Effects Models and Extensions in Ecology With R. Springer Science & Business Media.

Zuur, A.F., Ieno, E.N., Elphick, C.S., 2010. A protocol for data exploration to avoid common statistical problems. Methods Ecol. Evol. 1, 3–14.